Nano Today (2009) 4, 52—65

available at www.sciencedirect.com

ScienceDirect

journal homepage: www.elsevier.com/locate/nanotoday

REVIEW

Biomedical nanoparticle carriers with combined thermal and magnetic responses

Ting-Yu Liu[a,b], Shang-Hsiu Hu[b], Dean-Mo Liu[b], San-Yuan Chen[b], I-Wei Chen[a,*]

[a] *Department of Materials Sciences and Engineering, University of Pennsylvania, Philadelphia, PA 19104-6272, USA*
[b] *Department of Materials Science and Engineering, National Chiao Tung University, Hsinchu, Taiwan, ROC*

Received 18 September 2008; received in revised form 13 October 2008; accepted 13 October 2008

KEYWORDS
Nanoparticles;
Biomedical;
Thermal response;
Magnetic response;
Drug delivery

Summary Several biocompatible polymers are capable of large responses to small temperature changes around 37 °C. In water, their responses include shrinkage and swelling as well as transitions in wettability. These properties have been harnessed for biomedical applications such as tissue engineering scaffolds and drug delivery carriers. A soft material/hard material hybrid in which a magnetic metal or oxide is embedded in a temperature-responsive polymer matrix can combine the thermal sensitivity with magnetic signatures. Importantly, nanosizing such construct brings about new desirable features of extremely fast thermal response time, small magnetic hysteresis and enhanced magnetic susceptibility. Remote magnetic maneuvering and heating of the hybrid nanocolloids makes possible such applications as high-throughput enzyme separation and cell screening. Robust drug release on demand may also be obtained using these colloids and nanoparticle-derived thin film devices of combined thermal magnetic sensitivity.
© 2008 Elsevier Ltd. All rights reserved.

Introduction

Smart materials responsive to multiple environmental stimuli are of interest to biotechnology because of possible applications such as delivery carriers, separation platforms and environment sensors. Since body temperature is nearly constant, a small temperature excursion about it provides an environmental stimulus to be exploited. Temperature-responsive soft materials used in conjunction with localized heating (e.g., via hyperthermia) are therefore prime candidates for biomedical applications [1]. Other stimuli such as pH, glucose, stress or strain, and electromagnetic fields can be combined with thermal stimulus to create a multi-stimuli-responsive system. Here we focus on magnetic stimulus which can be applied remotely. One possible application of magnetically and thermally responsive smart nanomaterials is illustrated in Fig. 1 that pertains to remotely controlled drug delivery.

Since none of the soft materials suitable for biomedical applications is magnetic, a soft—hard hybrid construct is required to combine magnetic and thermal sensitivities. The soft temperature-responsive materials of choice are those

* Corresponding author.
E-mail address: iweichen@seas.upenn.edu (I.-W. Chen).

1748-0132/$ — see front matter © 2008 Elsevier Ltd. All rights reserved.
doi:10.1016/j.nantod.2008.10.011

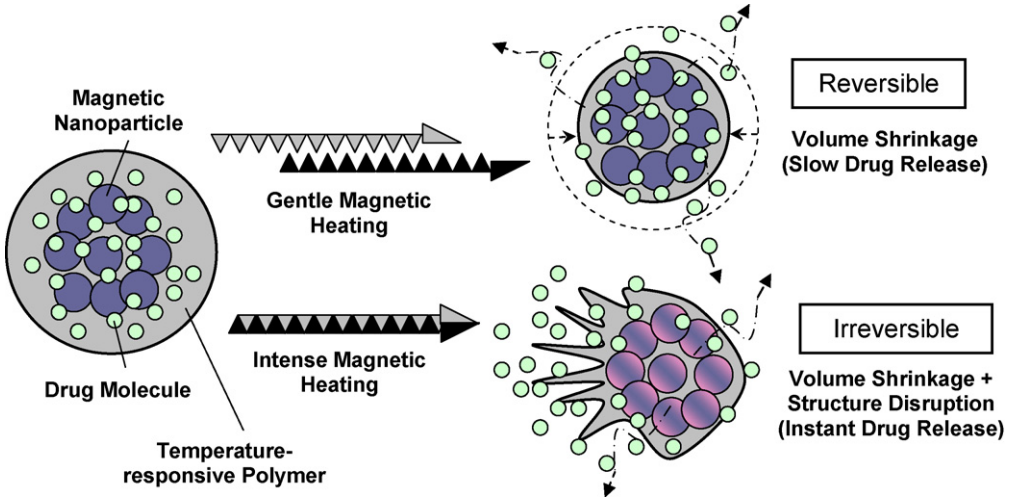

Figure 1 Two drug release mechanisms under magnetic heating. Gentle magnetic heating causes temperature-responsive polymer to shrink, squeezing drug out from the nanoparticle. Intense magnetic heating additionally ruptures the nanoparticle, triggering a burst-like drug release.

that form hydrogel [2], which is a three-dimensional network of polymer that retains its structure while being water absorbent; i.e., it swells, but does not dissolve, in water. Common biomedical uses of hydrogels include soft contact lenses made of silicone or polyacrylamide and medical electrodes made of polyethylene oxide. In some hydrogels, it is possible to couple water absorption and network deformation to a temperature-stimulated phase transition, so the temperature response may be manifested as a large change in the shape, rigidity, water content or hydrophobicity of the gel. The hard magnetic material of choice is iron oxide, which is relatively safe for biomedical applications and can be readily synthesized in a form of small particles to be embedded into the soft material. Iron oxide can be attracted to a magnet. Moreover, using a high-frequency field remote magnetic heating of iron oxide becomes possible thereby converting a magnetic stimulus to a thermal stimulus.

Nanotechnology offers several advantages to these materials. Nanoparticles of iron oxide do not have multiple domains found in larger magnets; the unit-cell spins of the entire nanoparticle line up and act as a single ''super'' spin that aligns more perfectly with the applied field giving rise to a higher magnetic susceptibility. This ''superparamagnetism'' unique to nanoparticles provides a stronger magnetic response than bulk magnetism. Meanwhile, breathing water in a temperature-responsive hydrogel is easier for nanoparticles because of shorter transport distance, so their response to a temperature stimulus is much faster than that of a bulk hydrogel. In addition, smaller hybrid particles form more stable colloids and they circulate better in the body; at the same time they can more easily penetrate and accumulate in the leaky, defective architecture of growing, vascularizing tumors [3,4]. Nanosized iron oxide and polymer particles can also be more readily digested in the body through biodegradation and clearance [5]. On the other hand, the stability of the nanoparticle construct and its cargo against chemical dissolution and degradation may be questionable. Moreover, the magnetic force on nanoparticle is very small because of small mass. In the following we will discuss the current status and understanding of the nanoscale hybrid systems which have been developed to exploit these thermal and magnetic responses for biomedical applications.

Temperature-responsive polymers

Like all materials polymers manifest thermodynamic structural transitions along with associated physical or chemical responses. These changes are categorized by the phase diagrams. Polymers, however, are unique in that their solutions may thermodynamically separate into two distinct phases at high temperatures, whereas in other materials such phase separations usually occur at low temperatures. Of special interest for biomedical applications is the behavior of a polymer—water solution which is stable below a so-called lower critical solution temperature (LCST), above which the solution partitions into two phases: water and a polymer-rich phase. This is in contrast to the phase separation below an upper critical solution temperature (UCST) that is more commonly encountered in non-polymer systems. Such LCST exists for both homopolymers and block copolymers. Some common ones are listed in Table 1.

Among the homopolymers that exhibit LCST, the most studied is poly(*N*-isopropylacrylamide) (poly(NIPPAm) or PNIPPAm) [6] (Fig. 2a) in which the LCST behavior represents a coil-to-globule transition in the shape of a hydrated polymer chain [7]. At low temperature, the chain solubilizes water which keeps the chain extended. At higher temperature, the lost entropy of the ordered water around the chain becomes energetically costly, so the water leaves for the bulk and the coil collapses under the hydrophobic force between polymer segments. Slightly crosslinked NIPPAm is therefore a thermally responsive hydrogel that shrinks above the LCST by rejecting water from the polymer network. Poly(*N*-vinylcaprolactam) (PVCL) is another extensively studied homopolymer with a similar LCST behavior [8].

Table 1 Thermal transitions of selected homopolymers, their modified copolymers, Pluronics®, synthetic elastin-like polypeptides and natural polymers.

Homopolymers		Modified copolymers		Pluronic® series and similar triblock copolymers		Natural polymers[a]	
Materials	LCST (°C)	Materials	LCST (°C)	Materials	CMT (°C)	Materials	$T_{gel-sol}$ (°C)[a]
Poly(*N*-isopropylacrylamide), PNIPAAm [71]	30—34	Poly(NIPAAm-co-AAm) [1,21]	35—55	L64 [12]	24—45	Gelatin/collagen [48,49]	~40
Poly(*N*-vinylcaprolactam), PVCL [2,71,74]	25—50	Poly(NIPAAm-co-*N*-tBAAm) [1]	<30	P65 [12]	26—49	Polysaccharides [2,86]	30—50
Poly(vinyl methyl ether), PVME [71]	37	PNIPAAm—PEG [77,78]	30—39	F68 [12]	27—53	Natural polymers[b]	
Poly(*N*,*N*-diethylacrylamide), PDEAAm [56,71]	25—34	PNIPAAm—CA—PCL [67]	37—38	P84/P85 [12]	19—47	*Materials*	$T_{sol-gel}$[b] (°C)
Poly(methacrylic acid), PMAA [2]	~75	PNIPAAm-b-PMMA/PBMA [79,30]	32—35	F88 [12]	22—53	Methylcellulose, MC [2]	~80
Poly(vinyl methyl oxazolidone), PVMO [2]	~65	P(NIPAAm-co-SMA) [80]	~40	P103/P104/P105 [12]	18—32	Hydroxypropylcellulose, HPC [2]	~55
poly(dimethylaminoethyl methacrylate), PDMAEMA [75]	~50	Poly(NIPAAm-co-DMAAm) [81]	32—44	F108 [12]	21—41	Polyphosphazene derivatives [2]	33—100
poly(*N*-(L)-(1-hydroxymethyl) propylmethacrylamide) [76]	~30	Poly(NIPAAm)-PL(G)A [68,69]	34—50	P123 [12]	13—26	Elastin-like polypeptides (ELPs)	
Poly(silamine) [2]	~37	poly(NIPAAm-co-HPMAm) series [82]	10—50	F127 [12]	20—36	*Materials*	*LCST* (°C)
Poly(siloxyethylene glycol) [2]	10—60	PUA-b-PNIPAAm [83]	~31	PEO—PLA—PEO [60]	19—32	Poly(GVGVP) [71,74]	28—30
Poly(vinyl alcohol), PVA [2]	~125	Peptide-modified P(NIPAAm-co-AAc) [84]	~34	PEO—PHA—PEO [85]	22—45	Poly(GVG(50% Val-30% Gly-20% Ala)P) [21,74]	40—42
Poly(vinyl pyrrolidone), PVP [2]	~160	PVCL-g-PTHF [2]	35—50	PEO—PEA—PEO [85]	14—44	Poly(GVG(6% Val-50% Gly-44% Ala)P) [21]	67

[a] Most natural polymers form a gel phase below $T_{gel-sol}$. At high temperatures, they have a random coil configuration forming a sol. At low temperature, renaturation to the triple helical conformation in gelatin and the double helical conformation in polysaccharides drives the formation of physical junctions, causing gelation.

[b] Some natural biopolymers (e.g., cellulose) undergo reverse thermogelation (gelation at elevated temperature from a sol state at low temperature) at $T_{sol-gel}$.

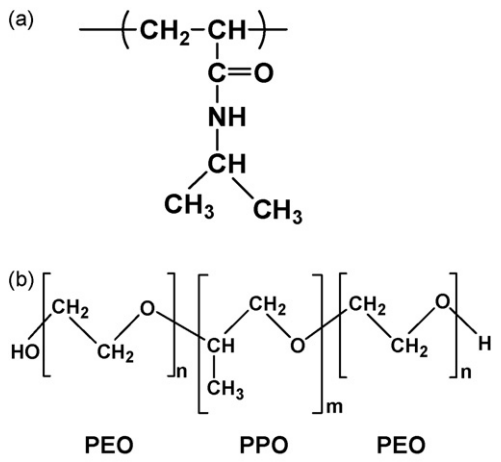

Figure 2 Chemical formula of two polymers that exhibit LCST. (a) PNIPAAm homopolymer and (b) PEO—PPO—PEO triblock copolymer.

Among block copolymers, the most studied are the poly(ethylene oxide)—poly(propylene oxide)—poly(ethylene oxide) (PEO—PPO—PEO) triblock copolymers [9] (Fig. 2b). PEO, also known as PEG, is frequently present as a biocompatible hydrophilic coating on nanoparticles to improve their *in vivo* circulation [10]; PPO, on the other hand, is more hydrophobic. Commercially known as Pluronics® (BASF) or poloxamers® (ICI) this amphiphilic polymer is a non-ionic surfactant because within each chain the PEO blocks and the PPO blocks can self-segregate into hydrophilic and hydrophobic domains, respectively. Above the LCST, interchain aggregation also occurs, forming alternating PEO and PPO layers arranged into micelles (with a hydrophobic PPO core and a hydrophilic PEO shell), cylinders, lamellas or other supramolecular structures [11]. In this sense, the LCST also represents the critical micellization temperature (CMT) [12—13]. Stabilized supramolecular structures of PEO—PPO—PEO (via chemical crosslinking, physical entanglement with another interpenetrating polymer network, or adsorption to a water/oil interface) undergo a volumetric transition at the LCST due to water solubilization/rejection in the PPO layer. Moreover, at higher concentrations swollen micelles may gel reflecting an ordering tendency akin to colloidal crystallization which maximizes the free volume, hence entropy, around individual micelles. Some PEO—PPO—PEO polymers listed in Table 1 have an LCST close to the physiological temperature (37 °C).

Natural biopolymers generally exhibit multiple structural transitions at increasing temperatures, some causing large shape changes. For example, a single strand polypeptide can reversibly transform from a helix to a coil above a characteristic temperature, and two helical strands of complementary DNA reversibly dissociate when heated above the ''melting'' temperature. Such changes of secondary and tertiary structures of natural biopolymers have a profound effect on their biological functionalities. The helix-to-coil transition is not the LCST type, however, unlike the coil-to-globule transition in PNIPPAm. This is because the conformation change from helix to coil [14] is mainly controlled by hydrogen bonding between amino acids (base pairs) and is relatively immune to the entropy-dominated influences of solubilization and hydrophobicity. So the UCST here is essentially the ''melting'' temperature of the hydrogen bond (between a carbonyl oxygen and an amine hydrogen). Synthetic block copolypeptides containing hydrophobic and hydrophilic blocks have also been synthesized to exploit their thermal responses. Hydrophobic blocks in these diblock and triblock copolypeptides typically appear as α-helices or β-sheets, whereas random coils serve as the hydrophilic blocks. However, unlike PEO—PPO—PEO block copolymers that form micelles, lamellas or other ordered supramolecular structures, the aggregation of hydrophobic blocks in these copolypeptides commonly leads to long range gelation forming an ''amorphous'' hydrogel instead [15,16]. For example, between two helices of the ''leucine zipper'' type the aggregation takes the form of side-wise lineup of the two helices, providing physical (as opposed to chemical) crosslinks for the gel [17]. The thermal behavior of these hydrogels is again the non-LCST type since they ''melt'' at high temperatures by breaking loose the crosslinks. Similar non-LCST behavior is found in natural hydrogels and some examples are listed in Table 1. When gelatin is cooled below the gelation temperature, random coils of polypeptides self-assemble into triple-helices of the collagen structure, providing crosslinks [18]. In this case, both hydrogen bonding and hydrophobic aggregation contribute to gelation.

Since any protein solution eventually precipitates at sufficiently high temperatures, hydrophobic collapse of the polypeptide backbone must be ultimately inevitable. Indeed, linear polypeptides made of monomers of a single amino acid species have a well defined collapse temperature which rises with the hydrophilicity of the respective amino acid: 24 °C for valine, 40 °C for proline, 45 °C for alanine and 55 °C for glycine [19]. Therefore, by combining different amino acids, it is possible to design linear homopolypeptides that hydrophobically collapse near the physiological temperature. These so-called ''elastin-like polypeptides'' (ELP) behave like PNIPPAm. For example, the LCST of an ELP made of Val-Pro-Gly-Val-Gly repeats is 26 °C [19], which is raised to 42 °C by randomly substituting 50% Val, 30% Gly and 20% Ala for the second valine in the repeats. Such ELP may be suitable for temperature-responsive drug delivery applications [20,21].

It is clear from the above discussion that the phase transitions and the associated property changes of the temperature-responsive polymers are fundamentally sensitive to the chemical and structural features of their building blocks as well as their surrounding [1]. This is unavoidable because the LCST transition reflects a delicate balance between solubilization and hydrophobic collapse, which involve electrochemical equilibrium and electrostatic/electrodynamic interactions. These influence-exerting features start with the primary structure of the polymer, including the hydrophilicity/hydrophobicity of the monomers and their arrangement (e.g., random copolymer versus block copolymer). They also extend to the secondary structure; for example, whether the hydrophobic block is a random coil, α-helix or β-sheet makes a difference [15—16]. Moreover, the chemistry and physical properties of the modifications to the polymer and its environment, including crosslinking agents, intentionally incorporated additives such drugs and imaging agents or unintentionally incorporated additives such as absorbed serum proteins, and the

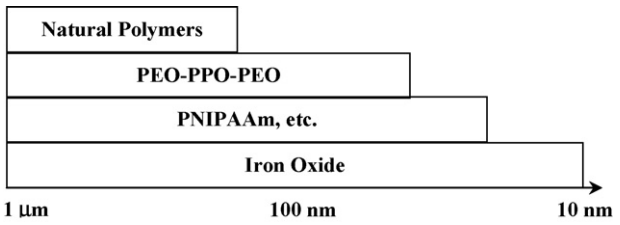

Figure 3 Size range of particles made of temperature-responsive polymers, as well as that of the iron oxide particles contained therein.

aqueous environment it is in (pH, salt concentration and dielectric constant), can all have a profound effect. Lastly, the molecular weight and polydispersity of the polymer are obviously important parameters as well. These factors should be taken into account in the design of any materials package involving temperature-responsive polymers.

Temperature-responsive nanocolloids

Although temperature-responsive polymers may be directly conjugated with drugs and used as such, a preferred form for controlled drug delivery entails the colloidal state in which the therapeutic substance is encapsulated inside the suspended nanoparticles [4]. Nanocolloids based on temperature-responsive polymers must remain stable in physiological electrolytes such as phosphate buffered solution (PBS) and serum. The typical size range of stable colloids prepared from common temperature-responsive polymers is shown in Fig. 3. Some examples of polymer-based temperature-responsive colloidal particles are given in Table 2.

Being an amphiphilic surfactant, PEO—PPO—PEO readily forms oil-in-water micelles with a PPO core and a PEO corona. Using double emulsion (water-in-oil-in-water) techniques (e.g., Fig. 4), one can also form PEO—PPO—PEO vesicles (liposomes or nanocapsules) with a shell made of a bilayer membrane that has hydrophilic, PEO-rich outer faces [22]. These colloids dilate below the LCST and shrink above the LCST, with a radius ratio typically ranging from 2 to 5 (Fig. 5). Post-formation crosslinking adds stability to the colloids without substantially affecting their thermal responses. The core of the PEO—PPO—PEO micelle can incorporate hydrophobic substance such as drug, as can the shell of the bilayer nanocapsule; meanwhile the core of the bilayer nanocapsule can be loaded with hydrophilic substance as illustrated in Fig. 4.

PNIPPAm is a homopolymer and does not self-assemble into micelles. However, latex-like colloids which exhibit volumetric responses to temperature changes can be prepared starting with NIPPAm monomers and proceeding with polymerization under emulsifying conditions that limit the reactions within emulsion micro-reactors. The product is often referred to as microgel [23,24] which may actually reach the nanosize (less than, say, 300 nm) for PNIPPAm [25] and PVCL [26]. More generally, PNIPPAm may be modified in two ways to become sufficiently amphiphilic, hence capable of self-assembly into nanocolloids [1]. First, when the NIPPAm blocks copolymerize with blocks that are more hydrophobic, the block copolymer self-assembles into micelles with a hydrophobic core and a PNIPPAm-rich corona. Conversely, when more hydrophilic pendants are added to NIPPAm, micelles form above the LCST with a PNIPPAm core and a hydrophilic corona; the micelles can then be crosslinked to maintain stability below the LCST. Triblock copolymer with both a hydrophobic end block and a hydrophilic end block can also be prepared [27]. A similar approach may be applied to form ELP colloids [20]. The above colloids also undergo volumetric transitions with a typical radius ratio ranging from 2 to 4, while their cores can again incorporate hydrophobic drugs.

The volume reduction of the colloid is obviously accompanied by water rejection. Accordingly, bulk or shell diffusivity may change significantly. In the case of hydrogel, there is evidence of a ''dry skin'' forming above the LCST that decreases the diffusivity [28,29]. Pronounced changes in surface properties are also experienced by some colloids. On colloids that have a PNIPPAm or ELP corona the surface switches from being hydrophilic to being hydrophobic as the LCST is exceeded, causing colloid to aggregate or even precipitate from the water solution [30]. The hydrophobic nanoparticles in the aggregate actually experience an addi-

Table 2 Volume changes and transition temperatures of colloidal particles made of temperature-responsive polymers. Volume change is generally larger for the Pluronic® series than for the PNIPAAm series. It also increases in the order of nanoparticles, microspheres/beads and nanocapsules.

Materials	Volume changes (%)	Transition temperature (°C)
PNIPAAm/iron oxide Beads [87][a]	~85	~35
PNIPAAm microsphere [88]	~83	~35
Au/Boltorn H_{40}-NIPAAm nanoparticle [89]	~64	~32
Pluronic® F127/iron oxide nanoparticles [90]	~78	20—25
Pluronic® F127 nanocapsules [91]	~97	~26
Pluronic® F127/heparin nanocapsules [22]	~99	~25
Pluronic® F127/poly(ethylenimine) nanocapsules [92]	92—97	~21
Au/Pluronic® F127 core—shell nanocapsules [93]	~96	~18
Pluronic® F127/PEG nanocapsules [94]	~89	~23
Pluronic® F68 nanocapsules [91]	~98	~40
Pluronic® F68/iron oxide nanocapsules [91]	~94	~40

[a] mm sized.

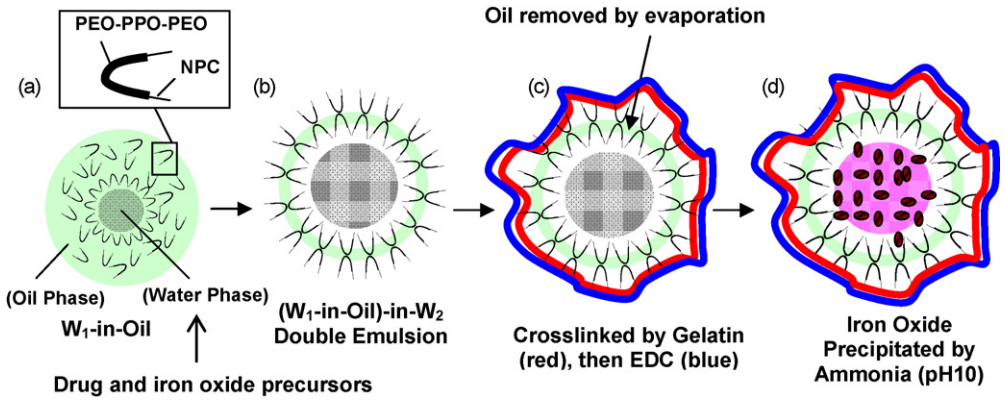

Figure 4 A self-assembly strategy of aqueous nanocapsules using two water phases and one oil phase for drug delivery under combined magnetic and thermal stimuli. ''W_1'': a water phase made of PBS into which a hydrophilic drug and Fe salts are dissolved. ''W_2'': a water phase made of PBS. ''Oil'': an oil phase made of methylene chloride solution containing PEO—PPO—PEO triblock copolymer (e.g., Pluronic® 68). The triblock copolymer is modified by reacting 4-nitrophenyl chloroformate (NPC) with PEO forming Pluronic®—NPC which can later react with gelatin for crosslinking. (a) Adding W_1 to oil forms an inverse micelle emulsion; (b) adding this emulsion to W_2 forms a liposome suspension containing nanocapsules with a bilayer PEO—PPO—PEO shell. (c) The PEO shell can be crosslinked by adding gelatin and held at 4 °C, and gelatin itself can be crosslinked by reacting with 1-ethyl-3-(3-dimethylaminopropyl)carbodiimide (EDC) at 4 °C; meanwhile, the oil residue in the PEO—PPO—PEO bilayer can be removed by evaporation. (d) Iron oxide nanoparticles can be precipitated by adding ammonia to raise pH to 10 under modest heating of 60 °C. The final F68 nanocapsule has a diameter of 108 nm at 25 °C and 43 nm at 50 °C (see Fig. 5).

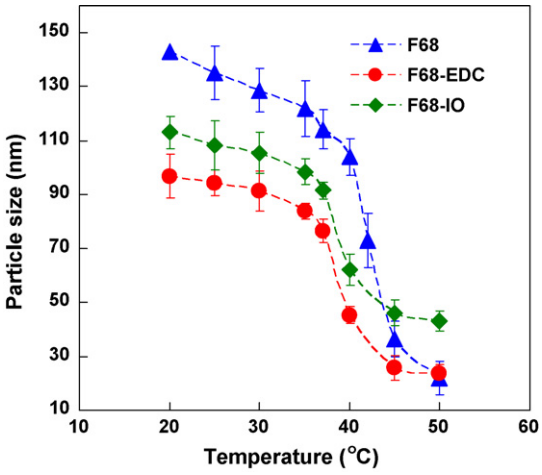

Figure 5 Temperature-responsive transition manifested by a diameter reduction above the LCST. F68 refers to nanocapsules having a shell made of a bilayer of the PEO—PPO—PEO triblock copolymer known as Pluronic® F68. Its structure is similar to that illustrated in Fig. 4(b). F68—EDC refers to similar nanocapsules in which the outer PEO shell is crosslinked by gelatin, which in turn is crosslinked by EDC. Its structure is similar to that illustrated in Fig. 4(c). F68—IO refers to fully crosslinked nanocapsules that additionally contain iron oxide nanoparticles in the core as illustrated in Fig. 4(d). The LCST may be identified with the inflection point of the size-temperature curve. The LCST is lower in F68—EDC and F68—IO mostly because the additive (NPC, see caption of Fig. 4), which reacts with PEO to render it crosslinkable, is less hydrophilic than PEO. Crosslinking constrains swelling at low temperature, so F68—EDC is smaller than F68 below the LCST. Filling the core with iron oxide nanoparticles further reduces shrinkage above the LCST.

tional squeeze caused by the inter-particle adhesion and osmotic pressure [30]. Such hydrophobic colloids have a strong tendency to adhere to the living cells. These changes do not occur on PEO—PPO—PEO colloids which have a PEO corona that is always hydrophilic.

Magnetic-core/shell

A magnetic-core or shell as a part of the colloidal nanoparticle offers three opportunities: the magnetic colloid can be attracted to the region of a high magnetic field H, it can experience an internal stress as non-uniform distortion arises from magnetic forces, and it can be heated by a non-contact magnetic field. The attracting field can be either DC or AC since the magnetic body force is the gradient of the magnetic internal energy density $1/2\chi\mu_0 H^2$, where χ is susceptibility and μ_0 is the permeability of vacuum. Therefore, high-susceptibility material is favored for magnetic localization. On the other hand, the heating field is always AC typically in the radio-frequency (RF) range, 10^4 to 10^5 Hz. Since an AC field can generate an eddy current, induction heating is always feasible for any conductor, but it becomes more efficient for a magnetic material in which magnetic hysteresis causes additional energy dissipation. To maximize the sum of eddy current (Joule) heating and magnetic heating, a relatively high electrical resistivity and large magnetic coercivity (mainly due to the resistance to domain wall movement) is therefore favored. However, nanomagnets suitable for nanocolloids are superparamagnetic [31], i.e., it is a single-domain ferromagnet free to switch following a quasi-static field without apparent coercivity. So there is little coercivity contribution and whatever energy dissipation must come from some sort of internal or boundary ''friction'' (see below) which does not prevent switching but nevertheless drags the magnetic moment

letting it lag the AC field. In a linear-response medium, the Debye theory describes this lag in terms of a relaxation time τ [32]. It then follows that maximal dissipation occurs when τ^{-1} is commensurate with the frequency f, i.e., $2\pi f\tau \sim 1$, because when $2\pi f\tau \ll 1$ there is no lag and when $2\pi f\tau \gg 1$ the moment stops to respond. Therefore, effective heating obtains by tuning the frequency to the range of $2\pi f\tau \sim 1$; under this condition more heat can be generated by driving the field harder (higher H) and faster (higher f). Lastly, magnetic distortion can be caused by either a DC or AC field as long as the frequency is not much higher than the resonance frequency. There is little knowledge of the magneto-mechanical resonance of colloidal nanoparticles although typical experiments utilizing magnetic distortion are conducted with a frequency much less than 10^3 Hz, a condition unlikely to contribute to much heating.

Among magnetic metals Co is perhaps the only material suitable for the magnetic-core or shell; Fe oxidizes too easily at the nanosize and Ni is toxic to the body. Among magnetic oxides iron oxide (IO) is preferred. Iron oxide takes the form of magnetite (Fe_3O_4) or maghemite (γ-Fe_2O_3), both having the structure of spinel although γ-Fe_2O_3 is a highly defected spinel containing many vacancies in the sublattices of both Fe^{3+} and O^{2-}. Maghemite IO is clinically used as a contrast agent for magnetic resonance imaging (MRI) because it causes a (dipolar-type) field inhomogeneity which accelerates the spin-spin relaxation/decoherence in its surrounding [33]. The use of other ferrites, such as magnetic spinels with other 3d transition metals partially substituting for Fe [34,35] and haxaferrites such as $BaFe_{12}O_{19}$ [36], is not advised because of increased complexity for synthesis and uncertain profile of toxicity.

Since all the above oxides are insulators, only Co may benefit from eddy current heating. However, no report exists for incorporating Co into nanosized temperature-responsive polymer colloid (Co-containing micelles made of other block copolymers have been reported [37]). The strategy to incorporate IO into the core of a temperature-responsive polymer colloid varies according to the nature of the core. In an aqueous solution, IO nanoparticles readily form from Fe(II) and Fe(III) salts at ambient or near ambient temperatures. After purification and recovery, the redispersed IO in an aqueous solution may be used as one part of the feedstock in the double-emulsion procedure to form the hydrophilic core of a PEO—PPO—PEO colloid (Fig. 4(a,b)). Alternatively, internal precipitation in the hydrophilic core which contains a Fe(II)/Fe(III) solution may be triggered by a pH increase after the formation of the colloid (Fig. 4(e)). For hydrophobic cores, hydrophobic IO nanoparticles need to be first synthesized, which typically involves high temperature precipitation in a long-chain alcohol such as oleic acid [38,39]. The oily IO can then be used in the emulsion procedure to enter the hydrophobic core. Since the procedure to grow spherical oily IO nanoparticles of a narrow size distribution from 3 to 20 nm (Fig. 6(a—d)) is rather well developed, it may also be used to prepare hydrophilic IO if it is modified with an additional step to introduce a hydrophilic outer coat using ligand exchange, physical adsorption or chemical conjugation [40,41]. Magnetic-shells containing IO are also possible. Since most shells of temperature-responsive polymer col-

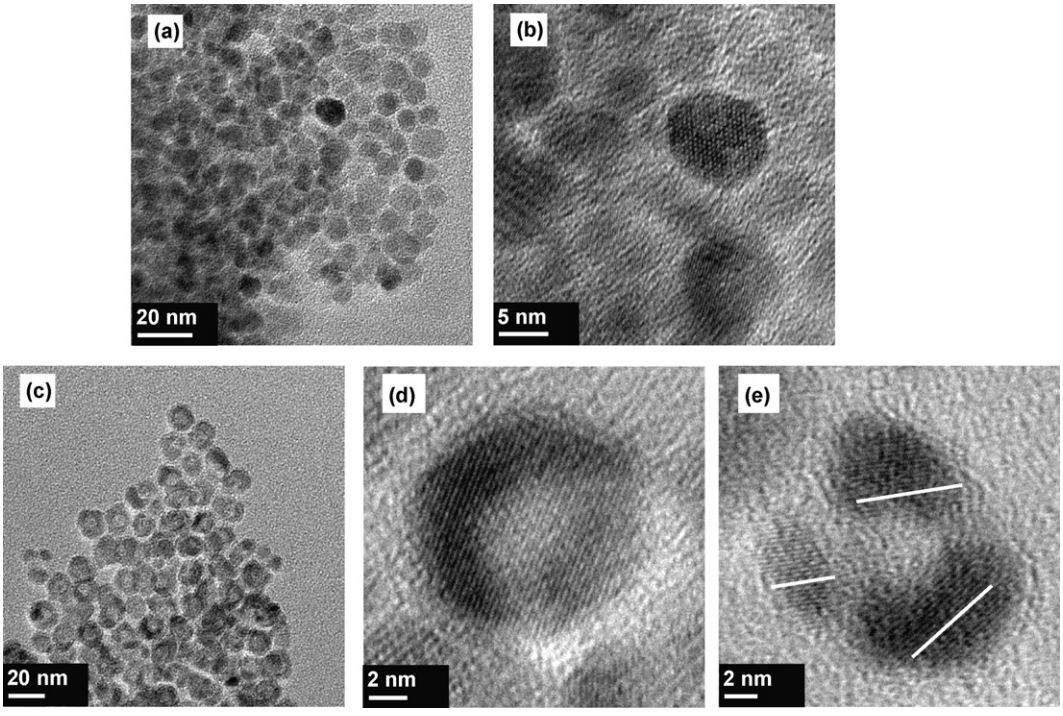

Figure 6 Morphologies, revealed by transmission electron microscopy, of iron oxide nanoparticles prepared from an oil-based solution. (a and b) are solid particles and (c and d) are hollow ones. The as-prepared nanoparticles are single crystals according to lattice imaging (b) and (d). (e) After magnetic heating, some hollow nanoparticles ruptured into pieces no longer in registry with each other, as indicated by markers.

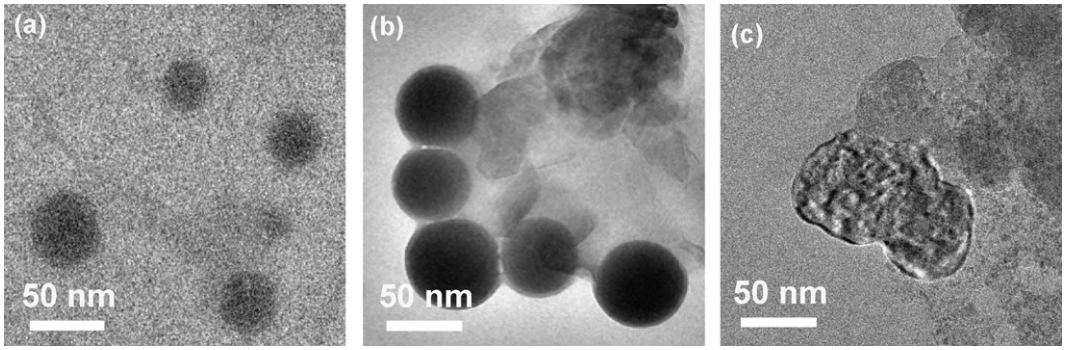

Figure 7 Transmission electron micrographs of F68—IO nanocapsules (see caption of Fig. 5) that show (a) uneven shrinkage after exposure to 45 °C, above the LCST. After magnetic heating, some nanocapsules ruptured (b), other coarsened into irregular shaped ones (c).

loids are hydrophilic, magnetic-shells are synthesized using hydrophilic IO. This is typically achieved by either adsorption of IO nanoparticles or precipitation from aqueous Fe precursors [26,42]. Using IO nanoparticles as seeds to initiate polymerization, other magnetic-core/polymer-shell nanocolloids can also be synthesized as reviewed by Schmidt [31].

Under magnetic heating the temperature of the magnetic nanocolloid solution gradually rises reaching a steady state of several to several tens of degrees of centigrade higher. At this temperature, the heat input from the magnetic nanoparticles equals the heat loss at the external boundary (the container, fixtures, surfaces). What is informative of magnetic dissipation is the initial heating rate, typically of the order of 0.1—1 °C/s for colloids containing IO nanoparticles. Since the energy input of the solution is entirely from the energy input of the magnetic nanoparticles, the initial heating rate of the nanoparticle should be precisely $C_W/C_M V_M$ times that of the (water) solution. Here C_W and C_M are the volumetric specific heat of water and the magnetic material, respectively, and V_M is the volume fraction of the magnetic material in the solution. Since $C_W/C_M \sim 1$ for IO and V_M is of the order of 10^{-3}, the initial heating rate experienced by the IO nanoparticle must be of the order of 10^2 to 10^3 °C/s. The steady state temperature of the IO nanoparticle depends on the heat exchange mechanisms between IO and the surrounding, which are currently unknown. However, microscopy evidence presented in Fig. 7 for IO nanoparticles in the core of a PEO—PPO—PEO colloid after RF heating suggests a rather high temperature of possibly several hundred degrees of centigrade. Clearly, very efficient ''frictional'' heating has been achieved. Magnetically caused fracture of hollow IO nanoparticles is also seen in Fig. 6(e), and similar transmission electron microscopy observations of magnetic-heat-rupture have been reported for silica nanoparticles coated with an (single crystalline) IO shell [43].

Assuming magnetic heating involves isolated, independent nanoparticles only, in an RF field friction arises in and around a magnetic particle from two sources [44]. First, particle may tumble causing frictional heating at the particle—water interface. The relaxation time τ_B for this mode can be estimated as the time required for Brownian motion over a characteristic distance of the order of one particle diameter. From Stoke—Einstein equation and viscous drag on a spherical particle, one can estimate $\tau_B = 3\eta V/kT$, where η is the viscosity at the interface, V is the particle volume and kT has its usual meaning. Brownian relaxation may not be responsible for the frictional heating of IO seen in Fig. 7, though, because the heat from this mechanism should be about equally shared between the nanoparticle and water so it is unlikely for IO alone to reach a very high temperature. Friction may also arise from spin rotation without crystal-lattice rotation. The relaxation time τ_N for this mode (Neel relaxation) is the reciprocal of the spin flipping rate which is of the order of $\nu_D \exp(-KV/kT)$. Here ν_D is the Debye frequency of the order of 10^{12}/s and KV is the energy barrier for coherent spin flipping which may be of a magnetocrystalline or shape origin. Most IO nanoparticles of several nanometers in size are superparamagnetic with a blocking temperature typically around 50 K or lower. At the blocking temperature, τ_N should be of the order of 10^{-2} to 10^2 s, so we estimate τ_N to be of the order of 10^{-10} s at room temperature. This would make Neel relaxation too fast to add to any significant friction in a RF field. However, the IO nanoparticles in Fig. 7 came from internal precipitation at the ambient temperature, so they are not perfect and most likely contain a high concentration of crystalline defects. Such defects may not significantly affect the blocking temperature and the superparamagnetic characteristics measured at low frequency, but they can greatly increase the friction against spin flipping thus causing lattice heating. This seems to be the most likely magnetic heating mechanism for the IO nanoparticles in Fig. 7.

Biomedical applications

Magnetically and thermally responsive nanocolloids may find applications in medicine and biotechnology such as drug delivery and enzyme immobilization/separation. Magnetic body force can align or relocate the colloid and magnetic dissipation provides a means of remote heating. Temperature excursions can trigger a change in the size, water content, diffusivity, surface properties and hydrogen bonding of the colloid. Although all of these individual effects have been separately illustrated in numerous studies, there are very few biomedically relevant reports that demonstrate the combined magnetic and thermal actions in the nanocolloid setting—bulk hydrogels and large (μm to mm) latex

particles are excluded. In the following, we summarize these studies and comment on the pertinent mechanisms.

Magnetic heating of UCST colloids

Conventional synthetic polymers may experience increased diffusivity and water content when magnetically heated above the UCST, which may accelerate the release of trapped drug or a model dye. This was reported by Schmidt and coworkers for an IO-core-containing poly(ε-caprolactone) (PCL) nanocolloid loaded with a solvatochromic dye; PCL exhibits an UCST of 35 °C when dispersed in dimethyl sulfoxide as in this study [45,46]. A more interesting study concerns a biopolymer with hydrogen bonding that melts above the UCST; magnetic heating then causes the release of hydrogen-bonded drug. This was demonstrated by Derfus et al. using IO nanoparticles to which single strand DNA was grafted: the DNA binds a dye-labeled complement below the UCST, then releases it above the UCST at the implanted site in a mouse tumor model [47]. Melting hydrogen-bonding in a bulk gel magnetically heated above the UCST has been used to increase the diffusivity, hence drug release from IO-containing collagen [48] and gelatin [49]. Extension to microgels of submicrometer sizes is in principle feasible but not yet reported.

Magnetic heating of LCST colloids

Magnetic heating of the NIPPAm colloid above the LCST induces aggregation and size shrinkage. Wakamatsu et al. [50] applied the first effect to IO-core/PNIPPAm-shell nanoparticles to trigger their entrapment in a column packed with hydrophobic beads. We have applied the second effect to PEO—PPO—PEO nanoparticles to squeeze out a hydrophilic drug from the core (the preparation method is shown in Fig. 4, size isotherm in Fig. 5, reconstructed magnetic-cores in Fig. 7, and the release mechanism in Fig. 1). This is the first example of utilizing magnetic heating and size shrinkage to control drug release from a nanocolloid. The profile of drug release rates shown in Fig. 8 is very favorable: very slow at 4 °C and 25 °C, modest at 37 °C (below the LCST), much faster at 45 °C (above the LCST) and bursting upon magnetic heating. Compared to an earlier example of μm-sized colloid (NIPPAm with IO) [51], the ratio of release under magnetic heating to that of 25 °C is at least a factor of 100 higher in this nanocolloid. A further comparison to other examples of magnetically triggered drug release (with or without a temperature-responsive polymer) is shown in Table 3.

Magnetic separation of LCST/UCST colloids

Magnetic support particles have been investigated for a long time as a separation platform in biotechnology. Nanometer sized colloids can reduce fouling, but magnetic separation becomes much more difficult because of the smaller magnetic force in comparison to colloidal forces that favor suspension and Brownian motion. Colloids made of LCST polymers aggregate above the LCST, so they experience a much larger magnetic force and smaller colloidal forces,

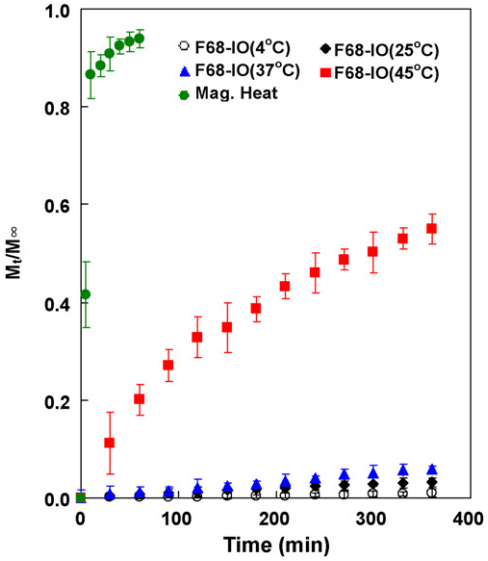

Figure 8 Cumulative release of a model drug (vitamin B_{12}) from F68—IO nanocapsules (see caption of Fig. 5) at various temperatures. The rapid increase from 37 to 45 °C is mostly due to nanocapsule shrinkage from 90 to 45 nm (see Fig. 5). The much faster burst-like release during magnetic heating is due to rupture of the nanocapsule (see Fig. 7).

thus allowing easy separation by a relatively low field. This has been demonstrated by Kondo and Fukuda [52] by heating IO-containing PNIPPAm colloids (150—250 nm) above 32 °C to separate immobilized enzymes on the nanoparticles. The dispersion-to-flocculation transition at the LCST was also utilized by the same group [53] to achieve magnetically aided affinity selection of target cells from phage display libraries. Similarly, magnetic separation of UCST colloids can be practiced below the UCST as illustrated by Kaiser [54] for IO-containing polystyrene nanoparticles. In the latter case, a hydrophobic solution (cyclohexane in this study) must be used.

Magnetic directing of LCST colloids

In vivo localization of nanomagnetic particles is feasible according to the study of Deng et al. [55] who localized IO-containing PNIPPAm nanoparticles (300—500 nm) to liver in a rabbit using a DC magnetic field; without a field accumulation in other organs (lung, spleen, kidney and heart) was observed. The colloid was initially placed below the LCST to access the swollen state to soak up doxorubicin, a hydrophilic drug for cancer treatment, although *in vivo* demonstration of drug release was not performed in this study apparently because the LCST (32—37 °C) is no higher than the body temperature. In principle, AC magnetic heating (hyperthermia) can also provide a localization effect for LCST colloids since above the LCST the colloid will precipitate with a tendency to adhere to the cells. Localized hyperthermia was proposed as a targeting tool to direct drug-loaded LCST colloids to tumors which are warmer (~42 °C) than the rest of the body [30], but this idea has not been demonstrated for magnetic colloids.

Table 3 Half-life (t_{50}) for drug release (typically a small molecule) from particles with and without magnetic heating. t_{50} is the time to reach $M_t/M_\infty = 0.5$, where M_t/M_∞ is the amount released at time t normalized by the total amount of drug contained (see Fig. 8). Much faster release with magnetic heating.

Materials	Half-time (t_{50})		Released molecules
	Without magnetic heating	With magnetic heating	
Pluronic® F68/iron oxide nanocapsules [91]	42 h (37 °C)/5 h (45 °C)	5 min	Vitamin B_{12}
Pluronic® F127/iron oxide nanoparticles [90]	18 h (15 °C)/3 h (45 °C)	5 min	Doxorubicin
Fe_3O_4/PAH capsules [95][a]	15 h (25 °C)	30 min	FITC—dextran
Silica/iron oxide nanospheres [43][a]	>20 days (25 °C)	3 min	Fluorescent dye
Silica/iron oxide nanospheres [96][a]	>10 days (25 °C)	15 min	Ibuprofen
Ethylene—vinyl acetate with embedded magnetic sphere [97][b]	Not measured (>40 days)	10 times shorter[b]	Bovine serum albumin

[a] Without a temperature-responsive polymer.
[b] 10 mm × 10 mm × 2 mm, not a temperature-responsive polymer, no magnetic heating, faster response due to magnetic distortion.

Membranes of magnetically and thermally responsive colloids

Various magnetic hydrogels not unlike those previously mentioned [48—49] have been studied but one serious shortcoming of the macroscopic gels is their slow response time, which scales with the size to the second power reflecting the diffusion limit of water transport [56]. This can be overcome if the macroscopic construct is itself made of nanoparticles of temperature-responsive hydrogel. Since the diffusion time of nanoparticle is very short, the response of the construct is also very fast despite its macroscopic dimension. Indeed, the nanoparticles can even be embedded in another gel without affecting the response time as long as water exchange in and out of the nanoparticles can proceed locally. One such construct with a magnetic signature is a membrane made by gelling nanoparticles or by depositing nanoparticle colloids. For example, Csetneki et al. reported a membrane made of nanoparticles with an IO-containing polystyrene core which is coated with PNIPPAm [57]. The membrane was endowed with a special microstructure by applying a magnetic field during gelation (below the LCST) with poly(vinyl alcohol) crosslinking: the magnetic nanoparticles are lined up into necklace strings due to dipole—dipole interactions. Above the LCST, shrunk nanoparticles disrupt the microstructure causing a rapid increase in permeability as demonstrated by bovine serum albumin penetration. Using spin coating, we have fabricated a 50-μm film of IO-containing PEO—PPO—PEO nanoparticles on a silicon substrate to demonstrate magnetically actuated rapid dye release from this device (Fig. 9). Micro-implant devices constructed in a similar way may be used for magnetically controlled drug delivery.

In vivo delivery

Hyperthermia via magnetically heating of IO has been studied in mice and human cadavers to treat breast tumors, showing tumor shrinkage and nuclear degenerations in heated malignant cells [58]. A maximum temperature elevation ΔT up to 88 °C was reported. A recent study demonstrated deep cranial thermotherapy using magnetic heating of aminosilane-coated IO applied to human glioblastoma multiforme patients who also received MRI and computed tomography (CT) for evaluation [59]. At a ΔT of 5—12 °C, patients reported no discomfort. For drug release, we already mentioned (see Magnetic heating of UCST colloids section) the study of fluorophore (a model drug) release from magnetically heated IO that was pre-implanted into a mouse tumor model [47]. Clinical use of dextran-coated IO as a MRI contrast agent has also been a well-established modality for liver imaging [33].

In the above applications IO colloids were delivered by direct injection to the target sites. In recent years, *in vivo* animal studies have been used to demonstrate the possibility of targeted delivery and imaging of IO with tethered targeting moieties; for example, folate ligand has been tethered to the dextran coating of IO via a linker to target tumor xenografts that overexpress folate receptors [60]. In theory, if the self-directed IO colloids are well localized to the targeted tumor site, they can also be magnetically heated to treat tumor, but this has not been demonstrated *in vivo*. Indeed, although multifunctional nanoparticles capable of targeted delivery of imaging agents and drugs is a much discussed concept, its *in vivo* demonstration for magnetic colloids is so far rare; we know of none for temperature-responsive magnetic colloids. In a recent review of application of nanotechnology in cancer therapy and imaging [61], only one was cited for simultaneous targeted delivery of drug and imaging agent: it delivers to targeted tumor cells small interfering ribonucleic acids (siRNA) that are covalently tethered to the dextran coating of IO [62]. This study did not utilize magnetic heating, magnetic directing or thermal sensitivity. Recently, Yang et al. used core-shell magnetic nanoparticles (core containing $MnFe_2O_4$, a spinel ferrite and doxorubicin, an anticancer drug) tethered with a breast-cancer-targeting antibody (human epidermal growth factor receptor 2 (HER2)) to simultaneously detect and treat cancer xenografts in mouse models [63]. Although this study used an amphiphilic block copolymer of poly(D,L-lactide-co-glycolide) (PLGA) and PEG

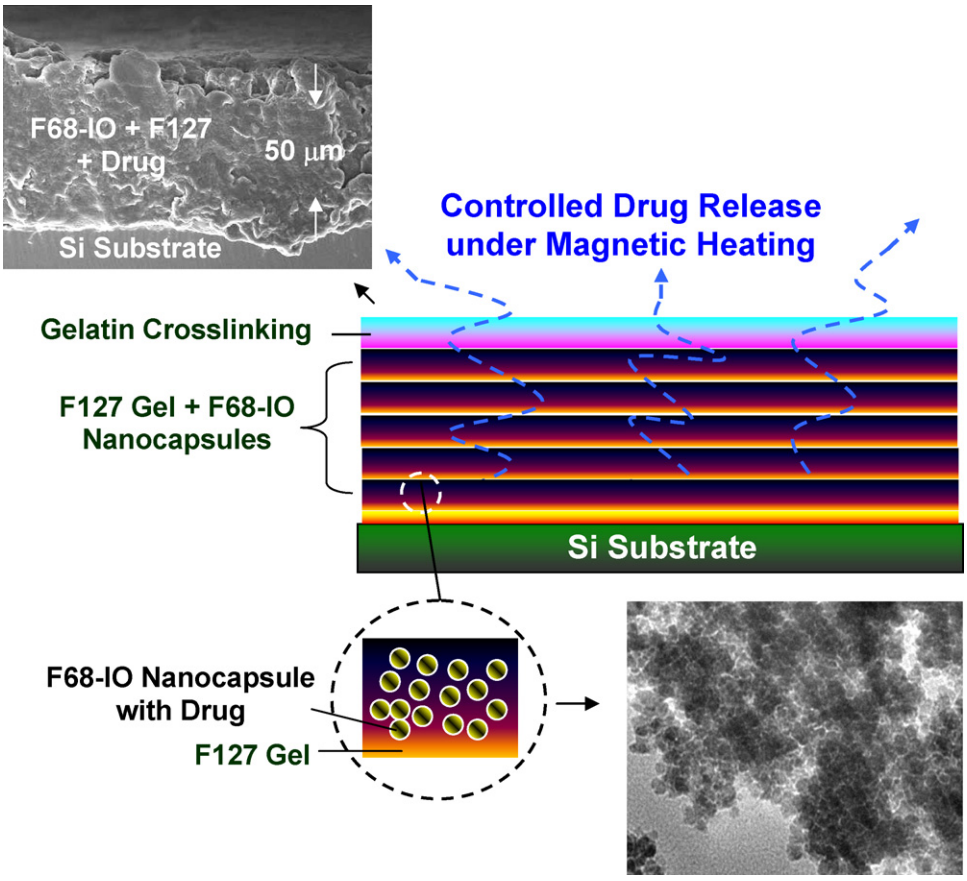

Figure 9 A device prototype made of iron-oxide-containing nanocapsules. Drug-containing F68—IO nanocapsules (see caption of Fig. 5) were spin coated onto a Si substrate to form a 60-μm thick film. Another PEO—PPO—PEO triblock polymer (Pluronic® F127) solution with a LCST of 22 °C was used in the spin-coating solution as a ''binder'' gel. After spin coating, a gelatin coating was introduced to crosslink the PEO shell of the nanocapsule. Magnetic heating triggers drug release from F68—IO. A similar implant device may be used for controlled drug release.

for the shell, which is not temperature-responsive, it should be possible to replaced PLGA—PEG by PEO—PPO—PEO or a PNIPPA copolymer. Using such a construct, functionalities of magnetic heating, magnetic directing and thermal sensitivity can in principle be incorporated into nanocolloid systems for self-directed simultaneous detection and treatment of diseases.

Designing nanoscale systems

We begin this section with a few comments on the drug release mechanisms in magnetically heated LCST colloids. Although a generic increase in diffusivity at higher temperature may play a minor role, the dominant mechanisms are all related to structural changes due to the LCST transition and magnetic field/heating. Clearly, the volumetric shrinkage provides a potentially powerful driving force for drug release from the core. Effective actuation requires core shrinkage, which is easier for a soft core than for a hard core [64]. However, volumetric shrinkage cannot account for the magnetically triggered burst-like release in Fig. 8, which is much faster than that achieved by heating to 45 °C (above the LCST) alone. The burst-like release is most likely due to the severe disruption of the IO core by magnetic heating. Other structural changes in the pore structure of the shell may also play a role. The changes may be caused by a thermal distortion akin to the one associated with a heated heterogeneous network structure: some regions expand while others contract. Magnetic forces may also cause a structural disruption of the shell when $2\pi f\tau_B \ll 1$, as shown in a low frequency (300 Hz) study on magnetically triggered on—off permeability switch across a polyelectrolyte shell surrounding a Co/Au core of 5 μm [65]. Force-directed structural movement is probably not important in the RF frequency range because, to effect shell distortion, $2\pi f\tau_B \ll 1$ must be satisfied for a particle of the size of the colloidal particle—a condition unlikely to be met.

We have already emphasized the importance of the LCST/UCST temperature, the structural transitions and the magnetic constituent of the nanocolloid that is responsive to both magnetic and temperature stimuli. For *in vivo* drug delivery, these temperatures should be a few degrees of centigrade above the physiological temperature, and preferably there is a large change in size and surface functionality. Tuning the transition temperature must be tackled

at the system level, since as mentioned before the transition temperature is sensitive to all chemical and physical aspects of the constituents of the polymer and its surrounding. A soft core is preferred to effect core shrinkage [64]. Actuation will be more effective if the transition temperature and the magnetic response are sharp. This requires a precise control of the composition and microstructure including a narrow distribution of the molecular weight of the polymer and of the size of the IO nanoparticles. Efficiency of magnetic heating is probably sensitive to the defect chemistry of the IO, its control and characterization at the nanoscale presenting a challenge. Cost, synthetic ease and scalability for mass production are important and mostly dependent on the chemistry and processes selected.

A successful system design should also address other issues of material chemistry and physics. First, safety and biocompatibility demand rigorous screening to eliminate any toxic chemical in the composition of the polymer and the process residue. A particularly complicated issue is colloidal and drug stability. Structural integrity of the nanocolloid obviously calls for substantial stability of the constituent polymer during storage and circulation, which may be improved by crosslinking. Nanocolloids tend to have longer circulation half-lives, but to help escape the fate of rapid clearance by macrophages or the reticuloendothelial system surface hydrophilic tethers of PEG or dextran (a polysaccharide) are beneficial [66]. Tethers may also reduce the absorption of serum proteins, thus avoiding enzymatic attack at the same time. Meanwhile, biodegradability of the temperature-responsive polymer would be desirable which may be introduced by incorporating biodegradable blocks or oligomers such as PCL [67], polylactic acid (PLA) [68] and PLGA [69], including their copolymers (in the PEO—PPO—PEO triblock copolymers, they should substitute for the PPO block) [60]. Concerning drug targeting, hydrophilic tethers mentioned above will mask the transition to hydrophobicity above the LCST of PNIPPAm and PVCL, so temperature-triggered aggregation and cell adhesion is no longer possible. In this regard, moieties for receptor or ligand bonding to enable targeted delivery is a desirable functionality that can be attached to the nanoparticles via suitable surface tethers [61]. Another important issue is the trigger for drug release. Although a long residence time after localization at the target site may sometimes be enough for delivering drug, a more efficient scheme is to utilize a device that allows for nanoparticle internalization (e.g., via receptor-mediated endocytosis) [70] and drug release (e.g., via an acid-labile linkage that is broken in the low-pH environment of endosomes) [71,72]. Lastly, drug loading is dictated by the physical chemistry of the polymer and the drug during fabrication, so a condition which simultaneously allows for polymer reaction (including self-assembly) and drug incorporation need to be found [64]. Since these aspects will again impact the transition temperature and transition characteristics, a system engineering approach must be adopted to find a satisfactory solution for this nanotechnology.

Finally, injection of particulate substance (liposomes, micelles and other natural or synthetic particles) in the submicron size range may elicit allergic reactions such as cardiovascular, respiratory and cutaneous symptoms, including death [73]. Typically, such reactions are most severe upon initial exposure, and the frequency of particulate allergy in the 5—45% range seems to be much higher than that of classical anaphylactic reactions to drugs (for example, penicillin allergy occurs in <2%). Interestingly, the trigger dose of hypersensitivity reactions in mouse models is two orders of magnitude higher than that in reactive man, so many animal studies may not foretell the threat of possible allergic reactions (Pig models appear to exhibit a similar trigger dose as reactive man). Therefore, designing safe nanoparticle delivery systems for *in vivo* applications may pose the most serious though least considered challenge.

Acknowledgements

This work was supported by the National Science Council of the Republic of China, Taiwan under contract No. NSC96-2627-B-009-006 and NSC96-2113-M009-027-MY2, and by the US National Science Foundation under grant No. DMR-05-20020 (MRSEC).

References

[1] E.S. Gil, S.M. Hudson, Prog. Polym. Sci. 29 (2004) 1173.
[2] B. Jeong, et al., Adv. Drug Deliv. Rev. 54 (2002) 37.
[3] G.J. Kim, S. Nie, Nanotoday August (2005) 28.
[4] I. Brigger, et al., Adv. Drug Deliv. Rev. 54 (2002) 631.
[5] E. Okon, et al., Lab. Invest. 91 (1994) 895.
[6] H.G. Schild, Prog. Polym. Sci. 17 (1992) 163.
[7] Y. Maeda, et al., Langmuir 16 (2000) 7503.
[8] V. Boyko, et al., Polymer 19 (2003) 8675.
[9] P. Alexandridis, T.A. Hatton, Colloids Surf. A 96 (1995) 1.
[10] S.M. Daly, et al., Langmuir 21 (2005) 1328.
[11] K. Mortensen, J. Phys.: Condens. Matter 8 (1996) A13.
[12] P. Alexandridis, et al., Macromolecules 27 (1994) 2414.
[13] P. Alexandridis, et al., Langmuir 11 (1995) 1468.
[14] A. Chakrabartty, R.L. Baldwin, Adv. Protein Chem. 46 (1995) 141.
[15] A.P. Nowak, et al., Nature 417 (2002) 424.
[16] J. Kopecek, Nature 417 (2002) 388.
[17] W.A. Petka, et al., Science 281 (1998) 389.
[18] A.G. Ward, A. Courts, The Science and Technology of Gelatin, Academic Press, New York, 1977.
[19] D.W. Urry, J. Phys. Chem. B 101 (1997) 11007.
[20] D.E. Meyer, et al., J. Control. Release 74 (2001) 213.
[21] A. Chilkoti, et al., Adv. Drug Deliv. Rev. 54 (2002) 613.
[22] S.H. Choi, et al., Langmuir 22 (2006) 1758.
[23] T.G. Park, A.S. Hoffman, Biotechnol. Prog. 10 (1994) 82.
[24] R. Pelton, Adv. Colloid Interface Sci. 85 (2000) 1.
[25] J. Rubio-Retama, et al., Langmuir 23 (2007) 10280.
[26] S. Bhattacharya, et al., Small 3 (4) (2007) 650.
[27] K.S. Soppimath, et al., Adv. Funct. Mater. 17 (2007) 355.
[28] T. Okano (Ed.), Biorelated Polymers and Gels, Academic Press, San Diego, CA, 1998.
[29] N.S. Satarkar, J.Z. Hilt, Acta Biomater. 4 (2008) 11.
[30] J.E. Chung, et al., J. Control. Release 62 (1999) 115.
[31] A.M. Schmidt, Colloid Polym. Sci. 285 (2007) 953.
[32] P. Debye, Polar Molecules, Dover, 1929.
[33] R. Weissleder, Radiology 193 (1994) 593.
[34] D.-H. Kim, et al., J. Magn. Magn. Mater. 293 (2005) 320.
[35] D.-H. Kim, et al., J. Magn. Magn. Mater. 320 (2008) 2390.
[36] P. Xu, et al., J. Phys. Chem. 111 (2007) 5866.

[37] J. Connolly, et al., J. Phys. D: Appl. Phys. 37 (2004) 2475.
[38] S. Sun, H.J. Zeng, J. Am. Chem. Soc. 124 (2002) 8204.
[39] S. Sun, et al., J. Am. Chem. Soc. 126 (2003) 273.
[40] J.-H. Lee, et al., Nat. Med. 13 (1) (2007) 95.
[41] J. Qin, et al., Adv. Mater. 19 (2007) 1874.
[42] S. Bi, et al., Mater. Lett. 62 (2008) 2963.
[43] S.-H. Hu, et al., Adv. Mater. 20 (2008) 2690.
[44] R.E. Rosensweig, J. Magn. Magn. Mater. 252 (2002) 370.
[45] A.M. Schmidt, J. Magn. Magn. Mater. 289 (2005) 5.
[46] A. Kaiser, et al., J. Phys.: Condens. Matter 18 (2006) S2563.
[47] A.M. Derfus, et al., Adv. Mater. 19 (2007) 3932.
[48] V.M. De Paoli, et al., Langmuir 22 (2006) 5894.
[49] S.-H. Hu, et al., Macromolecules 40 (2007) 6786.
[50] H. Wakamatsu, et al., J. Magn. Magn. Mater. 302 (2006) 327.
[51] D. Muller-Schulte, T. Schmitz-Rode, J. Magn. Magn. Mater. 302 (2006) 267.
[52] A. Kondo, H. Fukuda, J. Ferment. Bioeng. 84 (4) (1997) 337.
[53] H. Furukawa, et al., Appl. Microbiol. Biotechnol. 62 (2003) 478.
[54] Kaiser, J. Phys.: Condens. Matter (2006).
[55] Y. Deng, et al., Chem. Eur. J. 11 (2005) 6006.
[56] Y. Qiu, K. Park, Adv. Drug Deliv. Rev. 53 (2001) 321.
[57] H. Csetneki, et al., Macromolecules 39 (2006) 1939.
[58] I. Hilger, et al., Radiology 218 (2001) 570.
[59] K. Maier-Hauff, et al., J. Neuro-Oncol. 81 (2007) 53.
[60] S.W. Choi, et al., J. Polym. Sci. A 37 (1999) 2207.
[61] X. Wang, et al., CA Cancer J. Clin. 58 (2008) 97.
[62] Z. Medarova, et al., Nat. Med. 13 (2007) 372.
[63] J. Yang, et al., Angew. Chem. Int. Ed. 46 (2007) 8836.
[64] J.E. Chung, et al., J. Control. Release 65 (2000) 93.
[65] Z. Lu, et al., Langmuir 21 (2005) 2042.
[66] A.K. Gupta, M. Gupta, Biomaterials 26 (2005) 3995.
[67] W.-Q. Chen, et al., Polymer 49 (18) (2008) 3965.
[68] F. Kohori, et al., J. Control. Release 55 (1998) 87.
[69] S.Q. Liu, et al., Mol. Biosyst. 1 (2005) 158.
[70] S. Wang, P.S. Low, J. Control. Release 53 (1998) 39.
[71] D. Schmaljohann, Adv. Drug Deliv. Rev. 58 (2006) 1655.
[72] Z. Zhang, R.D.K. Misra, Acta Biomater. 3 (2007) 838.
[73] J. Szebeni, et al., J. Liposome Res. 17 (2007) 107.
[74] C. de las Heras Alaró, et al., Chem. Soc. Rev. 34 (2005) 276.
[75] H.S. Cho, et al., J. Polym. Sci. B: Polym. Phys. 35 (1997) 595.
[76] A.T. Muramaysu, et al., Macromolecules 34 (2001) 3118.
[77] Z. Yang, et al., Polymer 48 (2007) 931.
[78] M.D.C. Topp, et al., Macromolecules 30 (1997) 8518.
[79] H. Wei, et al., Biomaterials 30 (2007) 99.
[80] Y.A. Han, et al., Polym. Test. 21 (2002) 913.
[81] J.E. Chung, et al., J. Control. Release 53 (1998) 119.
[82] D. Neradovic, et al., Macromolecules 34 (2001) 7589.
[83] H. Wei, et al., J. Control. Release 116 (2006) 266.
[84] R.A. Stile, K.E. Healy, Biomacromolecules 2 (2001) 185.
[85] M.J. Song, et al., J. Polym. Sci. A 427 (2004) 772.
[86] E. Miyoshi, et al., Polym. Gels Netw. 6 (1998) 273.
[87] M. Zrínyi, Colloid. Polym. Sci. 278 (2000) 98.
[88] C.-J. Cheng, et al., Colloid. Polym. Sci. 286 (2008) 571.
[89] H. Xu, et al., Chem. Mater. 19 (2007) 2489.
[90] T.Y. Liu et al., Langmuir, in press.
[91] T.Y. Liu et al., Adv. Func. Mater., in press.
[92] S.H. Choi, et al., Biomacromolecules 7 (2006) 1864.
[93] K.H. Bae, et al., Langmuir 22 (2006) 6380.
[94] K.H. Bae, et al., Biomacromolecules 8 (2007) 650.
[95] S.-H. Hu, et al., Langmuir 24 (2008) 11811.
[96] S.-H. Hu, et al., Langmuir 24 (2008) 239.
[97] E.R. Edelman, et al., J. Biomed. Mater. Res. 19 (1985) 67.

Ting-Yu Liu (BS — Chemical Engineering, Yuan-Ze University, 2001; MS — Polymer Engineering, National Taiwan University of Science and Technology, 2003; PhD — Materials Science and Engineering, National Chiao Tung University, 2008) spent a year as Visiting Scholar in the Department of Materials Science and Engineering at University of Pennsylvania (2007—2008). He has authored over 20 papers on nanotechnology, polymer hydrogels and biomedical devices (dialysis and drug carriers). His current research interest includes ferrogels for drug controlled release and core—shell magnetic nanoparticles for targeted drug delivery and magnetic resonance imaging.

Shang-Hsiu Hu (BSc — Chemical Engineering, National Chung-Hsin University, Taiwan, 2004; MSc — Material Science and Engineering, National Chiao Tung University, Taiwan, 2006) is currently pursuing a PhD under the guidance of Prof. San-Yuan Chen. His research focus is on novel process development and controlled drug release in nano-biomaterial composites. He received National Innovation Award for Biotechnology and Medicine Industry (2007, 2008).

Dean-Mo Liu (MEng — Chemical Engineering, Chuan Yuan Christian University, Taiwan 86'; MSc — Materials Science, VPI&SU, USA, 1991; PhD Materials Science and Engineering, University of British Columbia, Canada 2004) joined National Chiao-Tung University, Taiwan as a professor of Materials Science and Engineering in 2007. Prior to that he spent 6 years in biomedical industry in Canada (2001—2007). His current research focuses on developing new (bio)materials and devices through colloidal-based assembly and biomimetic technologies. He has authored more than 150 technical papers and several scientific books. He has also served as a scientific advisory member for several technical journals and international conferences since 1998.

San-Yuan Chen (PhD, University of Michigan, Ann Arbor, USA, 1994) has been Professor of Material Science and Engineering at National Chiao Tung University of Taiwan since 1996. His current research is focused on functional photoelectronic inorganic nanomaterials, novel process development and controlled drug release in nano-biomaterial composites, and high-dielectric and ferroelectric memory thin-film processing. Honors include: National Innovation Award for Biotechnology and Medicine Industry (2007, 2008); Distinguished Engineering Professor Award from Chinese Engineering Institute (2005); Excellent Research Award from National Chiao Tung University (2003); Second-class Research Award from National Science Council (2005, 2006) and Marquis Who's Who in the World (since 2006).

I-Wei Chen (BS — Physics — 1972, Tsinghua; MS — Physics — 1975, Penn; PhD — Metallurgy — 1980, MIT) has been Skirkanich Professor of Materials Innovation at University of Pennsylvania since 1997. He taught at the University of Michigan (Materials) during 1986—1997 and MIT (Nuclear Engineering; Materials) during 1980—1986. He began ceramic research studying martensitic transformations in zirconia nanocrystals, which led

to studies on transformation plasticity, superplasticity, fatigue, grain growth and sintering in various oxides and nitrides. He is currently interested in nanograin ferroelectrics, nanoparticles for biomedical applications, nanostructured resistance memory devices and electromigration in fuel cells. A Fellow of American Ceramic Society (1991) and recipient of its Ross Coffin Purdy Award (1994), Edward C. Henry Award (1999) and Sosman Award (2006), he authored over 90 papers in the Journal of the American Ceramic Society (1986—2006). He received Humboldt Research Award for Senior U.S. Scientists (1997) and is a Chong-Kong Chair Professor of Tsinghua University in Beijing (2006—2009).